Dept. of Mech. Eng.
CUET

Published Online March 2019 (http://www.cuet.ac.bd/merj/index.html)

Mechanical Engineering Research Journal

Vol. 11, pp. 32–37, 2018

ISSN: 1990-5491

BOILING HEAT TRANSFER OF R134a FLOWING INSIDE A SMALL DIAMETER MICROFIN AND SMOOTH TUBE

M. K. Bashar[1*], Y. Ichinose[1], A. R. Tuhin[2], K. Kariya[3] and A. Miyara[3,4]

[1]Graduate School of Science and Engineering, Saga University, Saga, 840-8502, Japan
[2]Space Student, Saga University, Saga, 840-0024, Japan and Student, Department of Mechanical Engineering, Chittagong University of Engineering & Technology, 4349, Bangladesh
[3]Department of Mechanical Engineering, Saga University, Saga, 840-8502, Japan
[4]International Institute for Carbon Neutral Energy Research, Kyushu University, Fukuoka, 819-0395, Japan

Abstract: The boiling heat transfer coefficient of the refrigerant R134a inside a microfin (d_o = 2.5 mm) and smooth (d_o =2.5 mm) horizontal mini tube was experimentally investigated. The experiment has been carried out under the conditions of mass flux varying from 50 to 200 kg m^{-2}s^{-1}, the heat flux varying from 7 to 30 kW m^{-2}, over the vapor quality range of 0.0 to 1.0. The saturation temperature at the inlet of the test section was kept constant and it was equal to 13 ºC. The effect of mass flux, heat flux, vapor quality and tube fins on heat transfer coefficients have been analyzed. The boiling heat transfer coefficient showed a mass flux and heat flux dependency. The experimental results also showed that the microfin tube heat transfer coefficient was higher than that of the smooth tube for all mass flux ranges. Experimental results have been compared with well-known correlations.

Keywords: *Boiling, Heat Transfer Coefficient, Two-Phase Flow, Microfin Tube, Smooth Tube.*

NOMENCLATURE

AD = average deviation	[-]
d = diameter	[m]
G = mass flux	[kg m^{-2} s^{-1}]
h = enthalpy	[kJ kg^{-1}]
L = sub-section length	[m]
m = mass flow rate	[kg s^{-1}]
q = heat flux	[kW m^{-2}]
Q = heat exchange amount	[kW]
T= temperature	[°C]
x = vapor quality	[-]
Greek Symbols	
α = heat transfer coefficient	[kW m^{-2} K^{-1}]
η = heat balance	[-]
Subscripts	
eq = equivalent	
exp = experimental	
i = inner/inlet	
liq = liquid	
o = outer/outlet	
pre = predicted	
ref = refrigerant	
s = saturation	
v = vapor	
wi = inner wall	
w = water	

1. INTRODUCTION

Nowadays, microfin and smooth tubes exist in many applications ranging from different heat exchangers in the process industry to the automotive industry, HVAC, and domestic applications. Particularly, since the invention of microfin tubes has received a lot of attention because it can assure higher heat transfer coefficients compared to smooth tubes, with a relatively small increase of pressure drop [1]. However, a tube with hydraulic diameters smaller than 3 mm is generally considered to be a mini tube [2]. Mini microfin tubes are becoming popular as they can be used in the next generation of refrigeration and air-conditioning systems, leading to more

***Corresponding author:** Email: khairul.me08@gmail.com; Tel: +81 080-9064-0663

compact and more efficient heat exchangers. In addition, the use of these mini microfin tubes may imply a large reduction of the refrigerant charge of the system, thus squaring with the new stricter environmental regulations. Therefore, researchers have a strong interest in understanding the heat transfer characteristics of microfin mini tubes.

There are many studies on boiling heat transfer of R134a in horizontal smooth and microfin tubes in the open literature. Nevertheless, data regarding small diameter tubes (d_o<2.5mm) is scarce in the open literature. Some researchers who have analyzed different aspects related to boiling heat transfer inside microfin tubes are Kedzierski and Park [3], Mancin *et al.* [4] and Jiang *et al.* [5] etc. Choi *et al.* [6] carried out an experimental study on boiling heat transfer of R22, R134a and CO_2 in a horizontal smooth tube, having an inner diameter of 1.5 mm and 3.0 mm. The mass and heat fluxes ranged from 200 to 600 kg $m^{-2}s^{-1}$ and 10 to 40 kW m^{-2} respectively at a saturation temperature of 10 °C. Heat transfer coefficients were also compared to those of R22, R134a and CO_2. The heat transfer result shows heat flux and mass flux dependency. Regarding the tube diameter, Saitoh *et al.* [7] experimentally studied the boiling heat transfer mechanism of R134a in tubes with inner diameter of 0.51, 1.12, and 3.1 mm; they studied the effect of tube diameter and finally modified the Chen-type correlation. Kondou *et al.* [8] studied the flow boiling of R32, R1234ze(E), and R32/R1234ze(E) mixtures in a horizontal microfin tube with an inner diameter of 5.2 mm. Experiments were carried out at a saturation temperature of 10 ºC, heat fluxes of 10 and 15 kW m^{-2}, and mass fluxes from 150 to 400 kg m^{-2} s^{-1}. Results showed that, the mixture refrigerant had a lower heat transfer coefficient than both pure refrigerants. They were proposed a new correlation based on their experimental data. Daini *et al.* [9] experimentally studied the flow boiling of R1234ze (E) inside a microfin tube with an inner diameter at the fin tip of 3.4 mm. They compared heat transfer coefficient of R1234ze (E) with R134a. Wu *et al.* [10] performed flow-boiling experiments of R22 and R410A inside a microfin tubes with outer diameter of 5 mm.

However, this paper reports some results about R134a boiling heat transfer inside a small diameter smooth and microfin tube having an outer diameter of 2.5 mm at different operating conditions.

2. EXPERIMENTAL APPARATUS AND PROCEDURE

Figure 1 shows the schematic diagram of the experimental apparatus used in this study. The experimental test facility consists of a test section, refrigerant loop, cooling/heating water loop, sub-cooling loop and data acquisition system. The liquid refrigerant is pumped by an independently controlled gear pump magnetically coupled to a variable speed electric motor through, a filter, mixing chamber, pre-heaters, sight glass, test section, cooler and accumulator. The quality of refrigerant before entering the test section is controlled by the first pre-heater. The sub-cooled refrigerant then enters the test section to get experimental data in the vapor quality range of 0.1 to 0.98. Three mixing chambers are installed at the inlet of the first pre-heater and the test section and the outlet of the test section to measure the bulk temperature of the refrigerant. The system pressure of the test apparatus is controlled by the accumulator. The absolute pressure transducer, differential pressure transducer and K-type thermocouple at various positions and sight glass at the inlet and outlet of the test section are installed as shown in Fig. 1 to monitor the refrigerant's state. All of the signals from the pressure transducer and thermocouples are collected by a data acquisition system. The whole test apparatus were well insulated hence, it was not affected by the outside temperature.

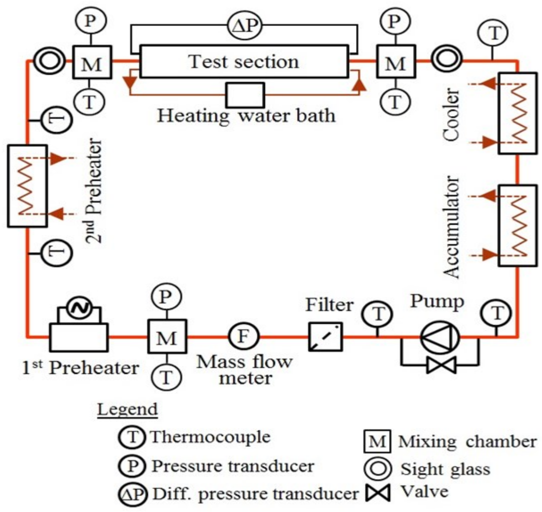

Fig. 1 Schematic diagram of experimental apparatus.

Figure 2 shows the schematic diagram of the test section for the present study. The test section consists of a horizontally installed copper tube, two headers and three water channels. The test tube is a small diameter microfin tube with an outer and equivalent diameter of 2.5 and 2.17 mm respectively. The parameters of the microfin test tube are as follows: number of fins 25, apex angle 31°, helix angle 10°, wall thickness 15 mm and fin height 0.1 mm. The outer and inner diameter of a smooth tube is 2.5 and 2.14 mm respectively. The total length of each test section is 852 mm and the effective heat transfer length is 744 mm. A differential pressure transducer with a calibrated accuracy of ±0.001 MPa is installed in the header to measure the pressure difference. The inlet and outlet refrigerant temperature are measured by two K-type thermocouples with calibrated accuracy of ± 0.03 °C installed in the inlet and outlet mixing chambers. The inlet and outlet pressure are measured by two pressure transducers with calibrated accuracy of ± 0.001 MPa inserted in the inlet and outlet mixing chambers. For measuring the inlet and outlet water temperatures, K-type thermocouples with calibrated accuracy of ±0.03 °C are also installed at the inlet and outlet of each sub-section. The heat balance factors of the most test runs are within ± 10% as shown in Fig. 3. The experiment was conducted over the mass and heat flux range from 50 to 200 kg m^{-2} s^{-1} and 7 to 30 kW m^{-2} respectively, vapor quality ranges from 0.1 to 0.98 and saturation temperature was 13 °C. The thermodynamic properties of R134a were obtained from REFPROP 9.1 [11].

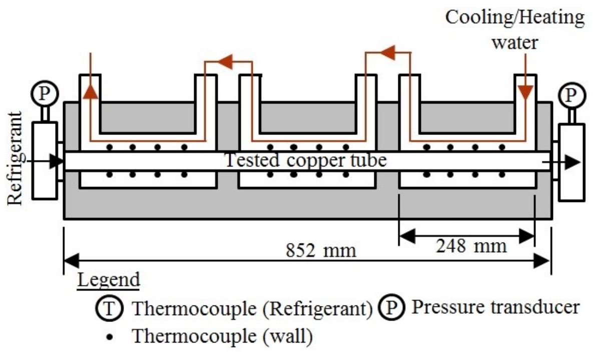

Fig. 2 Schematic view of the test section.

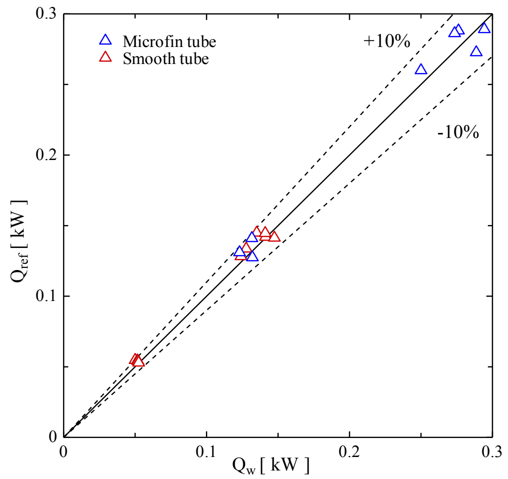

Fig. 3 Error in heat balance measurement of all the test runs.

3. DATA REDUCTION

The local heat transfer coefficient of each sub-section during the boiling was calculated by Eq. (1).

$$\alpha = \frac{q}{T_{wi} - T_b} \quad (1)$$

Where, α is the heat transfer coefficient, q is the heat flux, T_{wi} is the inner wall temperature and T_b is the bulk temperature that is the equilibrium saturation temperature. In this present experiment, the inner wall temperature was calculated from the measured outer wall temperature with a one-dimensional heat conduction equation. Therefore, the heat flux of each sub-section was calculated by Eq. (2). In this equation, d_{eq} is the equivalent diameter of the test microfin tube. Once the smooth tube d_{eq} was used in the experiment, it was defined by the inner diameter d_i.

$$q = \frac{Q_w \eta}{\pi d_{eq} L} \quad (2)$$

The heat balance factor η was calculated by Eq. (3).

$$\eta = \frac{Q_{ref}}{Q_w} \quad (3)$$

The heat gain of the refrigerant from inlet to the exit of the each sub- section was calculated by Eq. (4). Inlet and outlet enthalpy of the refrigerant in the test section were obtained from the REFPROP 9.1 at a measured refrigerant temperature and pressure of the corresponding point. The heat release of the water from the inlet to the exit of the each sub-section was calculated by Eq. (5).

$$Q_{ref} = m_{ref}\,(h_{ref,o} - h_{ref,i}) \quad (4)$$

$$Q_w = m_w(h_{w,o} - h_{w,i}) \quad (5)$$

The vapor quality in the test section was calculated by the following Eq. (6).

$$X = \frac{h_x - h_{liq}}{h_v - h_{liq}} \quad (6)$$

All experimental data was collected after the steady state was reached for temperature, pressure, and refrigerant flow.

4. RESULTS AND DISCUSSION

4.1. Experimental Results

The experimental data points of R134 for the microfin and the smooth tube are plotted on the Wojtan flow pattern map [12] where the data covers for a mass flux range of 50 to 200 kg m^{-2}s^{-1} and vapor quality range of 0.0 to 1.0, as shown in Fig.4. The flow pattern map has been drawn for a saturation temperature of 13°C. It can be seen from this flow pattern map that there is a slight variation in the transitional vapor quality X_{IA} between the intermittent flow and annular flow of mass flux 50, 100 and 200 kg m^{-2}s^{-1}, because X_{IA} is a function of density and viscosity ratio. However, at mass flux 200 kg m^{-2}s^{-1} for both tube, almost all the data points are lapped in intermittent and annular flow regime. Dry out is also found in the high vapor quality region for mass flux 100 and 200 kg m^{-2}s^{-1}, although dry out is not found at mass fluxes 50 kg m^{-2} s^{-1} for the smooth tube. At mass flux 50 and 100 kg m^{-2}s^{-1}, for both tubes some data points are lapped in slag and stratified wavy flow regime.

Figure 5 shows the experimental result of the heat transfer coefficient as a function of vapor quality at heat flux 13 kW m^{-2} and saturation temperature of 13 °C. It is seen that, for both tubes at the low mass flux of 50 kg m^{-2}s^{-1}, the heat transfer coefficient slightly increased with vapor quality and no dry out occur. On the contrary, at mass flux of 100 kg m^{-2}s^{-1}, the heat transfer coefficient remains almost constant for both tubes at a heat flux of 13 kW m^{-2}, up to a vapor quality of approximately 0.3, and then it increases with vapor quality, it reaches a maximum value and then suddenly decrease due to dry out phenomena. However, if mass flux is increased 2 times (i.e. 50 to 100 kg m^{-2} s^{-1}) for the smooth tube, heat transfer coefficient is increased about 1.06 to 1.45 times and heat transfer coefficient of the microfin tube is about 1.32-1.85 times higher than the smooth tube.

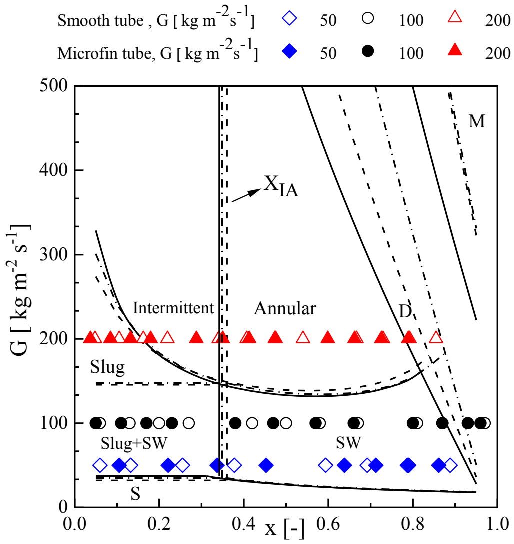

Fig. 4 Experimental data overlaid on the Wojtan flow pattern map.

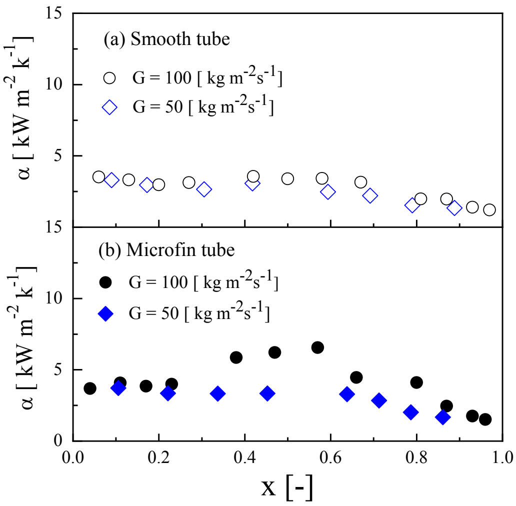

Fig. 5 Effect of mass fluxes and vapor quality on boiling heat transfer coefficient (a) Smooth tube (b) Microfin tube.

Figure 6 shows the comparison of the experimental and predicted heat transfer coefficient of 200 kg m^{-2} s^{-1} at heat flux 25 kW m^{-2} by Takamatsu *et al.* [13] correlation. The dash line represents the force convection (α_{cv}) heat transfer component, estimated by the correlation of Takamatsu *et al.* The solid line represents the prediction of the total heat transfer coefficient (α_{pre}), calculated by the same correlation. The difference between the predicted heat transfer coefficient and the force convection component denotes the nucleate boiling component (α_{nb}). However, this data trend can be explained considering the two competitive mechanisms that control the boiling phenomena: nucleate boiling and forced convection. For the smooth tube at low vapor qualities, nucleate boiling seems to be the controlling phenomenon, and no effect of vapor quality on the heat transfer coefficient is visible up to quality 0.3, when the vapor quality exceeds 0.4, the heat transfer coefficient increases with increasing vapor quality. Therefore, at high vapor quality region forced convection plays a more important role in the phase change mechanism. Furthermore, nucleate boiling component, α_{nb} is decreased in a noticeable degree for both tubes and the heat transfer coefficient is dominated by forced convection. This kind of similar experimental result is also reported by Diani *et al.* [14].

Figure 7 shows the effect of heat flux on the heat transfer coefficient and this Fig.7 plotted as the heat transfer coefficient against the vapor quality. It was seen that from this Fig. 7 the heat transfer coefficient increases with the heat flux increment. The Fig. 7 (a) is for the smooth tube; in this case, mass flux was kept at 50 kg m^{-2} s^{-1} and compared the measured results for two different heat fluxes: 7 and 13 kW m^{-2}. Increasing the heat flux from 7 to 13 kW m^{-2} shows that the heat transfer coefficient increases with heat flux up to quality o.8. The Fig. 7(b) is for the microfin tube, mass flux was kept at 200 kg m^{-2} s^{-1} and compared the measured results for two different heat fluxes: 25 and 30 kW m^{-2}, increasing the heat flux from 25 to 30 kW m^{-2} showed the heat transfer coefficient is almost same at the low-quality region and then it increases with vapor quality. Thus, in this case, the force convection boiling effect is more dominant than the nucleate boiling effect.

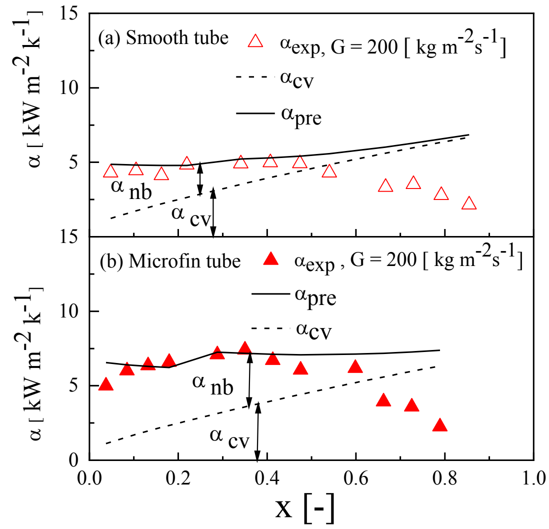

Fig. 6 Comparison of experimental and predicted heat transfer coefficient for mass flux 200 kg m^{-2} s^{-1} at saturation temperature 13 °C by Takamatsu *et al.* correlation (a) Smooth tube (b) Microfin tube.

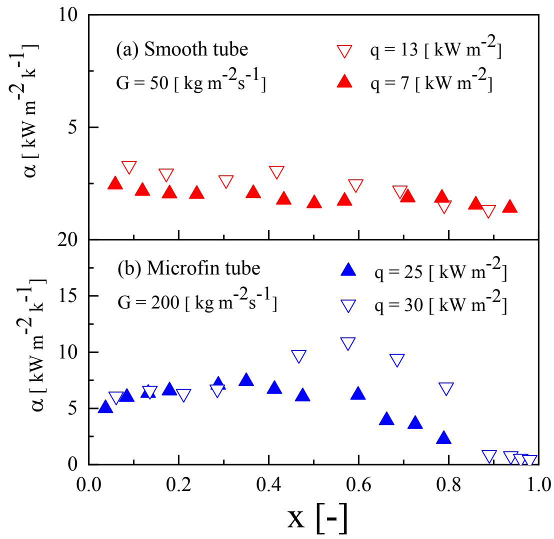

Fig. 7 Effect of heat flux on boiling heat transfer coefficient (a) Smooth tube (b) Microfin tube.

4.2. Comparison with Correlations

The experimental data was compared with two correlations to predict the boiling heat transfer coefficient. Two boiling heat transfer correlations were proposed by Choi *et al.* [6] and Saitoh *et al.* [7] as listed in Table 1. The first comparison, depicted in Fig. 8(a) shows the experimental data was predicted by Choi *et al*. [6]. This correlation was developed for a 7.75 mm horizontal smooth tube. This correlation also predicts the experimental data fairly well with a mean deviation (MD) of 26.740 % and average deviation (AD) of 26.740 %. Especially, about 90 % of the smooth tube data were predicted within ±30 %.

A Chen-type correlation for flow boiling heat transfer of R134a in a horizontal tube was modified taking into account the effect of tube diameter by Saitoh *et al.* However, this correlation captured the majority of the experimental data points; AD and MD are 10.910 %, 32.912% respectively as shows in Fig. 8(b).

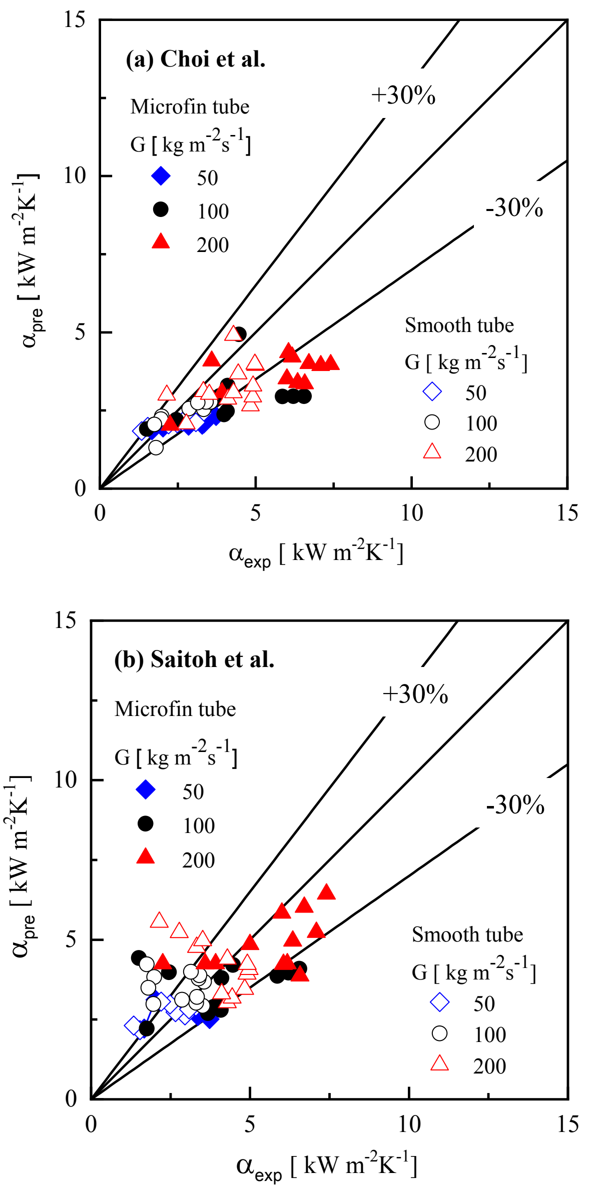

Fig. 8 Comparison of experimental heat transfer coefficient with correlations (a) Choi *et al.* [6] (b) Saitoh *et al.* [7].

Table 1 Correlations for predicting heat transfer coefficient

Author	Correlation
Choi *et al.* [6]	$\alpha_{tp} = E\alpha_1 + S\alpha_{SA}$, $\alpha_1 = 0.023 Re_l^{0.8} Pr_l^{0.4} \frac{\lambda_1}{d_i}$, $\alpha_{SA} = 207 \frac{\lambda_1}{d_b}\left(\frac{q d_b}{\lambda_1 T_{sat}}\right)^{0.674}\left(\frac{\rho_v}{\rho_l}\right)^{0.581} Pr_l^{0.533}$, $d_b = 0.0146\beta x[2\sigma/(g(\rho_1 - \rho_v))]^{0.5}$, $E = c_1 Bo^{c2} X_{tt}^{C3}, S = c_4 Co^{C5}$ Refrigerants: R32, R134a d_i = 7.75 mm G = 240-1060 kg m^{-2}s^{-1}
Saitoh *et al.* [7]	$\alpha_{tp,pre} = F\alpha_1 + S\alpha_{pool}$, $S = \left(1 + \alpha\left(Re_{tp} X 10^{-4}\right)^n\right)^{-1}$, $F = 1 + \frac{\left(\frac{1}{X_{tt}}\right)^2}{1 + We_v^m}$, $We_v = G^2 d_i/(\sigma\rho_V)$, $Re_{tp} = Re_l F^{1.25}$, $\alpha_{pool} = 207 \frac{\lambda_1}{d_b}\left(\frac{q d_b}{\lambda_1 T_{sat}}\right)^{0.745}\left(\frac{\rho_v}{\rho_l}\right)^{0.581} Pr_l^{0.533}$ Refrigerant: R134a d_i = 0.5-11 mm

5. CONCLUSIONS

The boiling heat transfer coefficient of R134a in a smooth and a microfin tube was measured experimentally and compared with two correlations. Different flow regime was observed using a flow pattern map. The heat transfer coefficients were measured at mass flux ranges of 50-200 kg m^{-2}s^{-1}, heat flux ranges of 7-30 kW m^{-2}, and saturation temperature of 13 °C. The results are summarized as follows.

(1) The boiling heat transfer coefficient of the microfin tube is about 1.32-1.85 times higher than the smooth tube.

(2) The boiling results show that the phase change mechanism is controlled by the nucleate boiling and two-phase forced convection. At low vapor quality (x<0.4), nucleate boiling heat transfer is the dominant heat transfer mechanism, and at high vapor quality, forced convective boiling is dominant.

(3) In the low vapor quality region for mass flux 50 kg m^{-2}s^{-1}, it was observed that a noteworthy influence of heat flux on the heat transfer coefficient while, in the high vapor quality region, this tended to vanish, and the heat transfer coefficient decreased. On the contrary, for mass flux 200 kg m^{-2}s^{-1}, increasing the heat flux this trend is the opposite because of an increased forced convection boiling effect.

(4) The prediction performance of the correlations was calculated by mean deviations (MD). The prediction performance of the correlations in ascending order is Saitoh et al., Choi et al. However, both of these correlations do not predict the microfin tube data well. Thus, it is necessary to develop a boiling heat transfer correlation for a small diameter microfin tube.

6. ACKNOWLEDGMENT

The authors would like to thank the Japan Copper Development Association for their financial support.

REFER ENCES

[1] K. Fujie, N. Itoh, H. Kimura, N. Nakayama and T. Yanugi, "Heat transfer pipe", US Patent 4044797, Assigned to Hitachi, 1977.

[2] S. G. Kandlikar, "Heat transfer mechanisms during flow boiling in microchannels", Journal of Heat Transfer, Vol. 126, pp. 8–16, 2004

[3] M. A. Kedzierski and K. J. Park, "Horizontal convective boiling of R134a, R1234yf/R134a, and R1234ze (E) within a micro-fin tube with extensive measurement and analysis details", National Institute of Standard and Technology Technical Note 1807, 2013.

[4] S. Mancin, A. Diani and L. Rossetto, "R134a flow boiling heat transfer and pressure drop inside a 3.4 mm ID microfin tube", Energy Procedia, Vol. 45, pp. 608–615, 2014.

[5] G. B. Jiang, J. T. Tan, Q. X. Nian, S. C. Tang and W. Q. Tao, "Experimental study of boiling heat transfer in smooth/micro-fin tubes of four refrigerants", International Journal of Heat and Mass Transfer, Vol. 98, pp. 631–642, 2016.

[6] K. Choi, A. S. Pamitran, Y. O. Chun and T. O. Jong, "Evaporation heat transfer of R32, R134a, R32/R134a, and R32/125/134a inside a horizontal smooth tube", International Journal of Refrigeration, Vol. 43, pp. 3651–3660, 2000.

[7] S. Saitoh, H. Daiguji and E. Hihara, "Correlation for boiling heat transfer of R-134a in horizontal tubes including effect of tube diameter", International Journal of Heat and Mass Transfer, Vol. 50, pp. 5215–5225, 2007.

[8] C. Kondou, D. Baba, F. Mishima and S. Koyama, "Flow boiling of non-a zeotropic mixtures R32/R1234ze(E) in horizontal microfin tubes", International Journal of Refrigeration, Vol. 36, pp. 2366–2378, 2013.

[9] A. Daini, S. Mancin and L. Rossetto, "R1234ze(E) flow boiling inside a 3.4 mm ID microfin tube", International Journal of Refrigeration, Vol. 47, pp. 105–119, 2014.

[10] Z. Wu, Y. Wu, B. Sunden and W. Li, "Convective vaporization in micro-fin tubes of different geometries", Experimental Thermal and Fluid Science, Vol. 44, pp. 398–408, 2013.

[11] E. W. Lemmon, M. L. Huber and M. O. McLinden, "Reference Fluid Thermodynamic and Transport Properties-REFPROP", Version 9.1, NIST Standard Reference Database 23, Gaithersburg, 2013.

[12] L. Wojtan, T. Ursenbacher and J. R. Thome, "Investigation of flow boiling in horizontal tubes: part I-A new adiabatic two-phase flow pattern map", International Journal of heat and mass transfer, Vol. 48, pp. 2955–2969, 2005.

[13] H. Takamatsu, S. Momoki and T. Fuji, "A correlation for forced convective boiling heat transfer of pure refrigerants in a horizontal smooth tube", International Journal of Heat and Mass Transfer, Vol. 36, pp. 3351–3360, 1993.

[14] A. Diani, S. Mancin and L. Rossetto, "Flow boiling heat transfer of R1234yf inside a 3.4 mm ID micro-fin tube", Experimental Thermal and Fluid science, Vol. 66, pp. 127–136, 2015.